

# Stochastic and deterministic switches in a bistable polariton micropillar under short optical pulses

A. V. Uvarov,<sup>1,2,3</sup> S. S. Gavrilov,<sup>3,4</sup> V. D. Kulakovskii,<sup>3,4</sup> and N. A. Gippius<sup>2,3</sup>

<sup>1</sup>*Moscow Institute of Physics and Technology, Moscow 117303, Russia*

<sup>2</sup>*Skolkovo Institute of Science and Technology, Skolkovo 143025, Russia*

<sup>3</sup>*Institute of Solid State Physics, RAS, Chernogolovka 142432, Russia*

<sup>4</sup>*National Research University Higher School of Economics, 101000 Moscow, Russia*

(Dated: March 13, 2022)

Optical bistability of exciton polaritons in semiconductor microcavities is a promising platform for digital optical devices. Steady states of coherently driven polaritons can be toggled in tens of picoseconds by a short external pulse of appropriate amplitude and phase. We have analyzed the switching behavior of polaritons depending on the pulse amplitude, phase, and duration. The switches are found to change dramatically when the inverse pulse duration becomes comparable to the frequency detuning between the driving field and polariton resonance. If the detuning is large compared to the polariton linewidth, the system becomes extremely sensitive to initial conditions and thus can serve as a fast random-number generator.

## I. INTRODUCTION

This study is concerned with the transient processes accompanying nonequilibrium transitions in bistable cavity-polariton systems. Polaritons are short-lived composite bosons that appear due to the strong coupling of cavity photons and excitons. They can form conventional Bose-Einstein condensates fed by the excitonic reservoir under nonresonant excitation conditions [1]. On the other hand, under direct resonant driving, they form highly nonequilibrium coherent states [2].

When the pump frequency *slightly* exceeds the polariton resonance frequency, the system has two or more steady states [3–6]. Their exact number depends on pump polarization because the interaction between polaritons is spin-sensitive: polaritons with parallel spins strongly repel each other. Varying excitation involves transitions between steady states, and a number of other switching mechanisms were proposed as well, based on short optical or acoustic pulses acting as switch triggers [7–10]. In the general case, the switch has the shape of a sharp jump followed by decaying transient oscillations. When their amplitude is small, their spectrum resembles above-condensate excitations in stationary Bose condensates [11–13]. In particular, when the blueshift of the pumped mode (condensate) equals the pump detuning and the lifetime is large, then the above-condensate modes have the Bogolyubov (sound-like) spectrum.

Here we study transient processes with particularly great intensities of nonlinear oscillations. The condensate is created by a continuous plane wave and disturbed by short-term optical pulses; for simplicity, we consider a circularly polarized system with only two steady states (“ON” and “OFF” for brevity) in a finite range of cw pump powers. A high-intensity switching pulse involves oscillations between these steady states and it becomes difficult to predict which of the two will be an eventual solution after the oscillations have decayed. We analyze this depending on the pulse parameters, its phase and

intensity.

Two different types of solutions exist. First, the pulse intensities resulting in the ON and OFF states can be tightly interlaced in the phase space. The intensity variation which is sufficient for altering the eventual steady state becomes infinitesimal as the polariton decay rate tends to zero. Thus, for a pulsed laser with a finite accuracy of repetition, this regime effectively enables a random number generation. The relative probabilities of the two outcomes are found to depend on the cw pump intensity.

The second type of solutions is, by contrast, completely deterministic. Within another area of the phase space, the system is guaranteed to be in the OFF state after the pulse has gone. The two types of solutions can coexist for the same set of the microcavity parameters. Therefore, the pulses with a “deterministic” outcome can be used to reinitialize the proposed random number generator. With increasing pulse power, stochastic and deterministic regions are well separated in the phase space but still alternate one after another.

## II. THE MODEL

### A. Gross-Pitaevskii equation

Polaritons in semiconductor microcavities are formed due to the strong interaction of cavity photons and two-dimensional excitons confined in quantum wells. This system is excited by a plane wave with frequency  $\omega_p$ . Polariton spectrum is split into two dispersion curves, lower and upper polariton branches:

$$\omega_{LP,UP} = \frac{1}{2} [\omega_{cav}(\mathbf{k}) + \omega_{exc}(\mathbf{k})] \mp \sqrt{(\omega_{cav}(\mathbf{k}) - \omega_{exc}(\mathbf{k}))^2 + \Omega_R^2}, \quad (1)$$

where  $\Omega_R$  is the Rabi splitting.

In order to localize polaritons at a certain place, the cavity mirrors can be etched out except the micropillar of a particular size. This approach allows one to confine polaritons while retaining a high  $Q$ -factor [14]. When the pillar has the radius of a few microns, the continuous spectrum is changed into a set of discrete energy levels due to size quantization. In planar cavities, the behavior of the macroscopic wave function  $\psi(\mathbf{r}, t)$  describing the polariton condensate obeys the Gross-Pitaevskii equation. The pillar can be represented by a deep potential well  $U(r)$ :

$$i\frac{\partial\psi}{\partial t} = (\omega_{LP}(-i\nabla) - i\gamma)\psi + U(r)\psi + V_a|\psi|^2\psi + f_a(\mathbf{r}, t)e^{-i\omega_p t}, \quad (2)$$

where  $V_a$  is the polariton repulsion energy per unit area,  $f_a$  is the pumping amplitude,  $\gamma$  is polariton decay rate (damping). The units of  $\psi$  are chosen so that  $[V_a] = 1$ . Here we assume that the pump is circularly polarized and neglect the spin degree of freedom.

This form of the equation is a simplified model, as we dropped the upper polariton branch and neglected the dependence of  $V_a$  on the wavevectors of the interacting waves. However, we believe that this simplification does not invalidate our conclusions because (i) the pumping frequency considered in this work is close to the lowest eigenstate, thus the upper polariton branch is energetically too far to have any significant influence, and (ii) the lowest eigenmode of the pillar contains the most of the wavefunction density, and it lies in the  $k$ -space area where the discrepancy caused by simplification of  $V_a$  is minimal. Hence, the error appears mostly in the other modes, which should not affect the result qualitatively. Nonetheless, one should keep in mind that such simplification effectively enhances the polariton-polariton interaction, and therefore it only gives the upper estimate of the impact of remote wavevectors.

The polariton system is known to exhibit bistable behavior if the pumping amplitude  $f$  is constant and the frequency detuning  $D = \omega_p - \omega_{LP}$  is larger than  $\sqrt{3}\gamma$ . The switching between such states is realized by adding a short pulse to the constant driving field:

$$f_a(\mathbf{r}, t) = \left( f_0 + f_1 \cdot 2^{-\frac{(t-t_0)^2}{2\tau^2}} \right). \quad (3)$$

Here  $f_1$  is complex-valued, so that it contains information about phase difference of cw pumping and the pulse:  $f_1 = |f_1|\exp(-i\phi)$ . The full width at half-magnitude (FWHM) of the pulse equals  $2\tau$ .

### B. Single-mode approximation of a micropillar

The core assumption underlying the single-mode approximation is that all other modes are sufficiently far from the pump frequency so that they do not affect the system behavior. Keeping that in mind and assuming

that pumping is monochromatic (i.e. the time dependence of  $f$  is much slower than the oscillations at the pump frequency), we introduce an ansatz:

$$\psi(\mathbf{r}, t) = \Psi(t)u_0(\mathbf{r})e^{-i\omega_p t} + \chi(\mathbf{r}, t), \quad (4)$$

where  $u_0$  is the normalized wavefunction of the ground state in a circular potential well,  $\chi$  denotes the deviation of the solution shape from that of the ground state and is assumed to be small compared to the first term. Such an ansatz corresponds to exciting the system with a very weak pump, so that the nonlinear term can be neglected. Substituting (4) into (2) and projecting it on  $u_0$  yields a single-mode equation for  $\Psi$ :

$$i\frac{\partial\Psi}{\partial t} = (-D - i\gamma)\Psi + V|\Psi|^2\Psi + f, \quad (5)$$

where  $V = V_a \int |u_0|^4 dS$ ,  $f = \int u_0^* f_a dS$ .

## III. SINGLE-MODE APPROXIMATION

### A. Reaction to the pulse

In the absence short-term pulses, equation (5) is autonomous. Its typical phase portrait is depicted in Fig. 1. The two steady states are stable foci (labeled as ON and OFF), while the unstable state is a saddle point (S). The  $\Psi$  phase plane is shown by the trajectories according to their final state and shows the basins of attraction of two steady states.

Now let us consider the system excited with a short pulse which then relaxes to one of two steady states. Naturally, the resulting state depends on the properties of the pulse. This problem has three characteristic time scales: the decay time  $\gamma^{-1}$ , the pulse duration  $\tau$ , and the inverse frequency of rotation in the phase space,  $T = |-D + V|\bar{\Psi}|^2\bar{\Psi}|^{-1}$ , where  $\bar{\Psi}$  denotes a characteristic value of  $\Psi$ , e.g. its average absolute value during the pulse. The solution changes the most noticeably upon varying the ratio between the last pair of characteristic times, whereas  $\gamma^{-1}$  is assumed to largely exceed both of them. If  $\tau \ll T$ , the solution does not propagate too far in the transverse direction during the pulse. With sufficient accuracy, the pulse can be replaced by the delta function. Since the frequency depends on  $|\Psi|^2$ , this approximation is valid only in a finite interval of amplitudes. Its validity is also limited by the uncertainty relations: if the pulse is short, its spectral width is high, thus the pulse will necessarily affect the eigenstates beyond the first one.

On the contrary, if  $\tau \gg T$ , then the driving field and phase plane change slowly, while  $\Psi$  evolves relatively fast. If, in addition,  $\tau$  is comparable with  $\gamma^{-1}$ , the solution follows the equilibrium state adiabatically. In this case, the final state depends on how the system leaves the bistability region during the pulse. If the pump power is beyond the bistability turning point, the OFF state merely vanishes, and thus the system can be reliably delivered to the

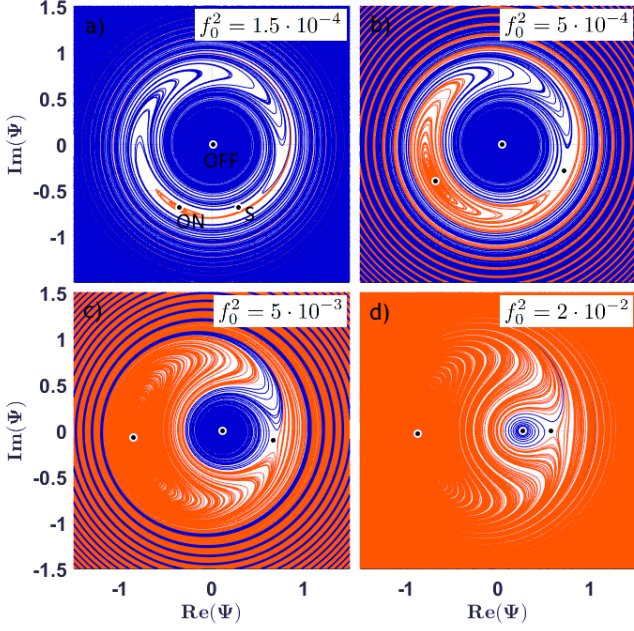


FIG. 1. Phase plane for equation (5) with time-independent pumping amplitude. Trajectories shown by red and blue curves are attracted to the ON and OFF states, respectively. Points highlight the stationary solutions: ON, OFF, and  $S$ . Here and in all other figures, unless stated otherwise,  $\hbar D = 0.6$  meV,  $\hbar\gamma = 0.014$  meV,  $V = 1$ .

ON state. The only exception occurs when the phase difference between the background cw pump and the pulse approximately amounts to  $\pi$ . Here the two pump sources cancel each other and the overall intensity drops down to quite a low value before it restores back to the cw intensity. As a result, the system is reliably delivered to the OFF state. This regime is consistent with switching discussed in Ref. [9].

Now let us consider the regime when  $\tau \sim T$ . During the switching pulse, one can imagine an instant phase plane with instant steady states and their basins of attraction. The absolute value of the ON point moves rapidly at the leading and back fronts of the pulse and slows down near the pulse maximum. Due to the strong blue shift of the resonance at high powers,  $\Psi_{ON}$  grows as a cubic root of the pumping amplitude. As a result, during the switching pulse, the solution rotates around the slowly drifting ON state corresponding to the instantaneous magnitude of the total external field. After the switching pulse has turned off,  $\Psi$  gradually returns to one of the stationary states following the flow lines of the stationary phase plane.

This switching regime can be illustrated by the example of a rectangular switching pulse  $f_1$  turned on during a certain time  $\tau$ . The solution rotates around  $\Psi_{ON}$  with negligible decay, and after the pulse has turned off, the solution goes along the stationary phase trajectories. If for two pairs  $(f_1, \tau)$  the angle spanned by the solution

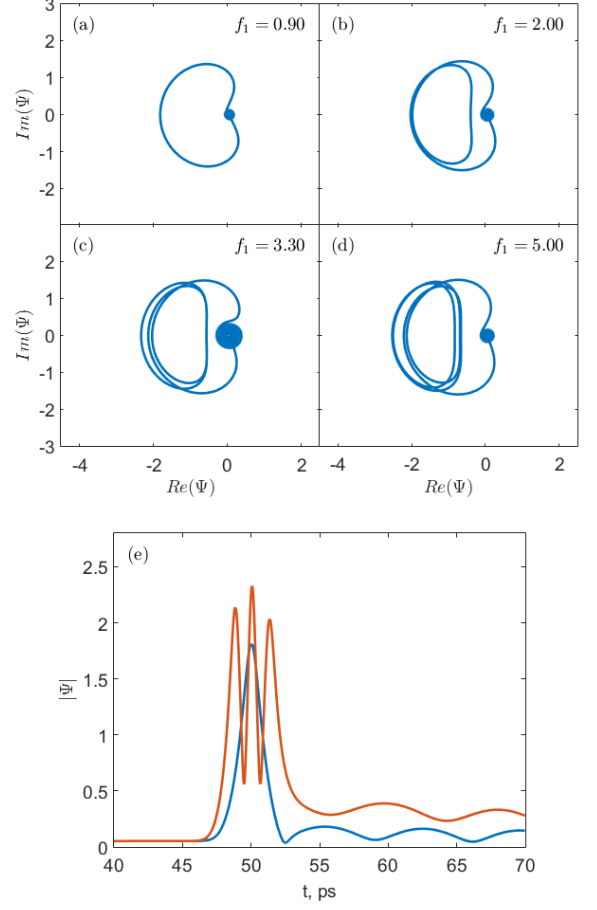


FIG. 2. (a) - (d): Four different trajectories that leave the system in the OFF state. (e): trajectories for  $f_1 = 0.9$  (blue) and  $f_1 = 3.3$  (orange) versus time. Despite making several loops with high  $|\Psi|$  during the switching pulse, all these trajectories converge to the OFF state. Note as well that the central point of such rotations changes slowly compared to the pulse amplitude  $f_1$ . The FWHM of the pulses is 2 ps.

around the ON point is the same up to  $2\pi$  (see an example of such trajectories on fig. 2), the resulting trajectories are the same and these pairs can be considered equivalent. The angular velocity of such rotation can be estimated by considering a perturbed solution near the ON state:  $\Psi = \Psi_{ON} + \delta\Psi$ . If we substitute this into (5) and keep only the terms no smaller than  $\delta\Psi$ , we get

$$i(\delta\dot{\Psi}) = (-D - i\gamma)\delta\Psi + V(|\Psi_{ON}|^2\delta\Psi + \Psi_{ON}^2\delta\Psi^*). \quad (6)$$

Let  $\delta\Psi = re^{i\theta}$ ; then, after separating the real and imaginary parts of the equation, we obtain

$$\dot{r} = V\text{Im}(\Psi_{ON}^2 e^{-2i\theta})r - \gamma r; \quad (7)$$

$$\dot{\theta} = (D - 2V|\Psi_{ON}|^2) + V\text{Re}(\Psi_{ON}^2 e^{-2i\theta}). \quad (8)$$

The latter equation suggests that in the case of a very strong pumping, the solution rotates clockwise (that is,

$\dot{\theta} < 0$ ), and  $-3V|\Psi_{ON}|^2 < \dot{\theta} < -V|\Psi_{ON}|^2$ . Taking into account that, asymptotically,  $|\Psi_{ON}|^2 \sim f_1^{2/3}$ , we have  $|\dot{\theta}| \sim |f_1|^{2/3}$ . If the solution has made a full circle around the  $\Psi_{ON}$  point, i.e.  $2\pi n = \tau \dot{\theta} \sim \tau f_1^{2/3}$ , the corresponding trajectories are equivalent. Thus, to estimate the amplitudes of the equivalent switching pulses in the phase space, we should solve this equation for  $f_1$ , which eventually gives  $f_1^{(n)} \sim n^{3/2}$ .

## B. Simulation results

We simulated the response of the single-mode system to the pulses discussed above. Each set of the initial conditions and other system parameter results in one of two states, ON and OFF, which can be indicated by different colors on the phase plane. The result of such mapping can be seen in Fig. 3. In the series of subplots, the pulse duration increases from left to right. The leftmost panel shows the final states in the case of very short pulses. Such a short pulse makes the system evolve along the straight line (that is why the look of the  $f$  plane resembles the  $\Psi$  plane, drawn in accordance with the basins of attraction). The rightmost panel shows the other extreme condition. Here the different sectors of the plane almost do not mix with each other, because the solution follows the “equilibrium” adiabatically. When  $f_1$  is aligned in phase with the cw pumping, the OFF state becomes unavailable, and so the solution sticks with the ON state. When  $f_1$  is aligned against the cw pumping, there is a time interval when the ON state is unavailable, so the system returns to the OFF state. The fact that the system is still non-adiabatic manifests itself in the serrate border of the regions: the transient oscillations do not smooth out completely during the pulse. The longer the lifetime, the more pronounced the serrate area of the phase space (see Fig. 4).

The middle panel shows the final states for the intermediate pulse length. This picture exhibits a small region in the middle where the characteristic spiral unwinds counterclockwise and then back again. This behavior is consistent with the explanation suggested above. With increasing  $|f_1|$ , the trajectories firstly get to higher values of  $|\Psi|$ . Then the growth stops (as the rotation establishes) and after the pulse the value of  $|\Psi|$  decreases. Finally, at certain  $|f_1|$ , the system arrives in the vicinity of the OFF state, regardless of the relative phase  $\phi$ . That is the reason for the dark ring in seen in the Figure. This pronounced ring-shaped area belongs to the OFF basin, and as long as the trajectory ends up close to zero, the result does not depend on the relative phase of the pulse. However, with the increasing the background cw pumping the OFF basin shrinks and moves off-center, which leads to the gradual disappearance of the ring (see fig. 5). It is important to note that the coloring repeats itself indefinitely, albeit with some transverse distortion. Again, this is predicted by the model of the solution revolving

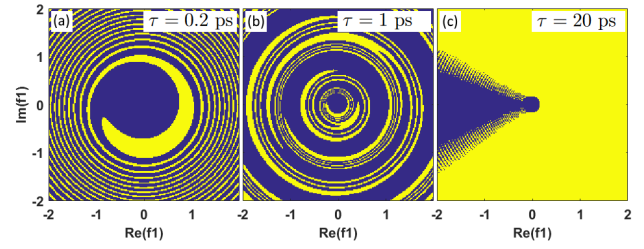


FIG. 3. Final state of the single-mode system as a function of complex amplitude of the pulse. Starting state is OFF. Different panels show the result for different  $\tau$ .  $f_0^2 = 5 \cdot 10^{-4}$ . All other parameters are fixed and equal to those in fig. 1.

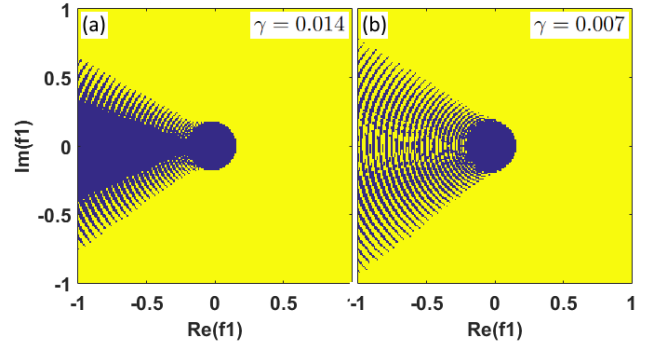


FIG. 4. Serrate edge of the regions in the  $f_1$  plane changes with different decay ratio.

around the instant equilibrium.

The smaller the decay ratio, the more rotations the solution makes before arriving into the saddle point and “scattering” into the vicinity of a certain focal point. In the sense of Fig. 7, this means more “coils” in the diagram. The rest of the diagram stays more or less stable, including the ends of the spirals, the ring with the guaranteed OFF state, etc.

In the limit of  $\gamma \rightarrow 0^+$ , there is a certain region where the density of the “coils” tends to infinity (fig. 6). In this regime, the system effectively becomes a random number generator unless the pump power is known with an infinite accuracy. In general, this generator is biased to one of the two states depending on the background pump pa-

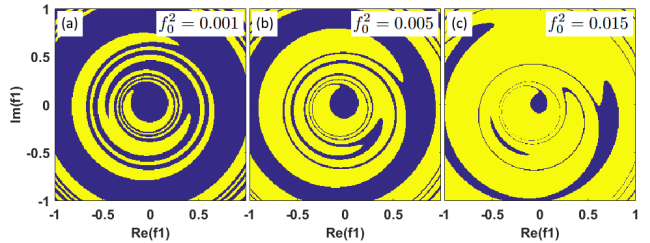


FIG. 5. Evolution of the middle panel in fig. 3 under gradual increase of the background cw pumping.

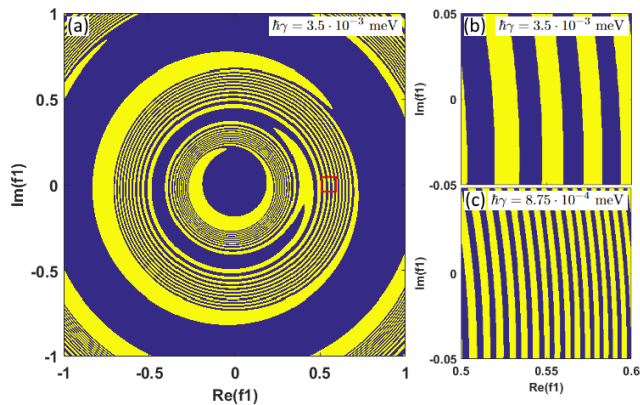


FIG. 6. (a): Final states diagram for a value of  $\gamma$  much smaller than other characteristic times of the system. Panels (b), (c) magnify the area highlighted with the red square, for different values of the decay parameter.  $\tau = 1\text{ps}$ ,  $f_0^2 = 5 \cdot 10^{-4}$ .

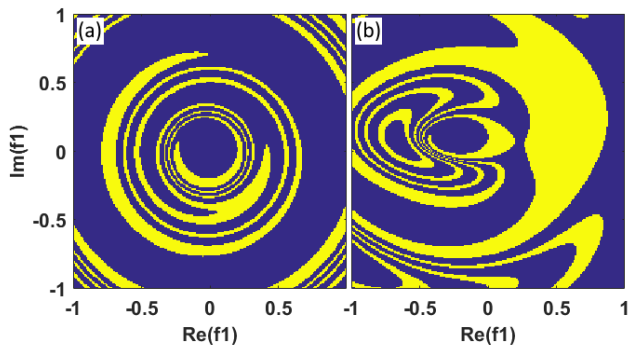


FIG. 7. Final states of the system (after the pulse) in the cases when the starting state is OFF (a) and ON (b).  $f_0^2 = 0.0005 \text{ meV} \cdot \text{ps}^{-2}$ , pulse FWHM = 2 ps.

rameters. This opens a way to manipulate the relative probability of the outcomes. Surprisingly, in the phase space, this regime coexists with the completely deterministic regime.

The approach developed above can be applied to the single-mode system in the ON state as well. When the system is in the ON state, the pulse can drive it down or leave in the ON state, depending on the pulse parameters. However, since the ON state is substantially off-center in the phase diagram (Fig. 1), there is no analog of the “belt” that is seen when the system is initially in

the OFF state (see fig. 7, (b)). Thus, if we were to send the system to the OFF state, we could apply the pulse with the amplitude from that belt. Such pulses can drive the system down or leave unchanged, but they definitely cannot drive it up. Thus, if we cannot control the phases of the pulses, we still can send a train of pulses and guarantee that the system is sent down after a certain number of them.

#### IV. CONCLUSIONS AND OUTLOOK

We have studied the driven polariton mode under the joint action of cw and pulsed pumping when the system is bistable and the short pulse acts as a trigger of transitions between steady states. The result is shown to be a nontrivial function of the pulse duration and amplitude. Depending on these parameters, several dynamical scenarios can be distinguished.

First, for sufficiently small decay rate, there is a region of pumping amplitudes where any point is within a small distance from both basins of attraction. Second, there is a region of large pumping amplitudes where the transition from the OFF state to the ON state is forbidden for any pulse phase. The combination of these two effects can be used to make a random-number generator: first, in response to the short pulse the system goes to one of two states that cannot be predicted in view of finite accuracy, and, second, the system can be reinitialized by the pulses whose amplitudes are guaranteed to not switch the system into the ON state. However, such a device would require a long lifetime of polaritons and correspondingly slow rate of transitions.

At the first glance, the polariton oscillator behaves similarly to a two-level quantum system under pulsed excitation which experiences the Rabi oscillations. However, the two-level system periodically passes through both excited and ground states, while the discussed polariton oscillator orbits the ON state and does not pass through the low-intensity OFF state during the pulsed excitation.

#### V. ACKNOWLEDGEMENTS

The work was supported by the Russian Science Foundation (Russian Federation) (Grant No. 14-12-01372). The images in this work were prepared using MATLAB [15].

[1] H. Deng, H. Haug, and Y. Yamamoto, *Reviews of Modern Physics* **82**, 1489 (2010).  
 [2] V. F. Elesin and Y. V. Kopaev, *Soviet Physics JETP* **36**, 767 (1973).  
 [3] A. Baas, J. P. Karr, H. Eleuch, and E. Giacobino, *Physical Review A* **69**, 023809 (2004).  
 [4] T. K. Parařso, M. Wouters, Y. Léger, F. Morier-Genoud, and B. Deveaud-Plédran, *Nature Materials* **9** (2010).

[5] A. Amo, T. C. H. Liew, C. Adrados, R. Houdré, E. Giacobino, A. Kavokin, and A. Bramati, *Nature Photonics* **4**, 361 (2010).  
 [6] S. S. Gavrilov, N. A. Gippius, S. G. Tikhodeev, and V. D. Kulakovskii, *Journal of Experimental and Theoretical Physics* **110**, 825 (2010).  
 [7] S. S. Gavrilov and N. A. Gippius, *Physical Review B* **86** (2012).

- [8] M. Klaas, H. Sigurdsson, T. C. H. Liew, S. Klemmt, M. Amthor, F. Hartmann, L. Worschech, C. Schneider, and S. Höfling, *Physical Review B* **96** (2017).
- [9] W. L. Zhang, F. Wang, Y. J. Rao, R. Ma, and X. M. Wu, *Journal of Lightwave Technology* **33**, 3933 (2015).
- [10] R. Cerna, Y. Léger, T. K. Paraïso, M. Wouters, F. Morier-Genoud, M. T. Portella-Oberli, and B. Deveaud, *Nature Communications* **4** (2013).
- [11] A. S. Brichkin, S. G. Tikhodeev, S. S. Gavrilov, N. A. Gippius, S. I. Novikov, A. V. Larionov, C. Schneider, M. Kamp, S. Höfling, and V. D. Kulakovskii, *Physical Review B* **92** (2015).
- [12] S. S. Gavrilov, A. S. Brichkin, Y. V. Grishina, C. Schneider, S. Höfling, and V. D. Kulakovskii, *Physical Review B* **92**, 205312 (2015).
- [13] D. Solnyshkov, I. Shelykh, N. Gippius, A. Kavokin, and G. Malpuech, *Physical Review B* **77**, 045314 (2008).
- [14] C. Schneider, P. Gold, S. Reitzenstein, S. Höfling, and M. Kamp, *Applied Physics B* **122**, 19 (2016).
- [15] MATLAB, *Release 2016b* (The MathWorks Inc., Natick, Massachusetts, 2010).